Field dependence of the longitudinal muon polarization for anomalous muonium

D. W. Cooke, M. Leon, and M. A. Paciotti
Los Alamos National Laboratory, Los Alamos, New Mexico 87545

P. F. Meier
Physik-Institut der Universität Zürich, CH-8057, Zürich, Switzerland

S. F. J. Cox
Rutherford Appleton Laboratory, Chilton, Oxon OX11 0QX, United Kingdom

E. A. Davis
Department of Physics and Astronomy, University of Leicester, LE1 7RH, United Kingdom

T. L. Estle and B. Hitti
Department of Physics, Rice University, Houston, Texas 77251

R. L. Lichti
Department of Physics, Texas Tech University, Lubbock, Texas 79409

C. Boekema and J. Lam
Department of Physics, San Jose State University, San Jose, California 95192

A. Morrobel-Sosa
California Polytechnic State University, San Luis Obispo, California 93407

J. Oostens
Science Department, Lindsey Wilson College, Columbia, Kentucky 42728

(Received 23 March 1994)

An unusual longitudinal-magnetic-field dependence of the muon polarization for anomalous muonium (Mu^*) in polycrystalline semiconductor targets is predicted, and has been observed for Si. As a function of field, the experimentally measured muon polarization at 53 K exhibits a cusp, i.e., a discontinuous jump in the slope from negative to positive, at 340(5) mT, in good agreement with theory. This occurs because the effective field on the μ^+ vanishes at this external field as the angle between it and the Mu^* symmetry axis approaches 90°. At 200 K no cusp is seen because Mu^* has been thermally annihilated. Fractional populations of the different muonium species are derived from the 53-K data. All Mu^* and other anisotropic centers, including molecular radicals, should exhibit such a cusp, allowing the possibility of observing such species even in disordered or amorphous solids where spectroscopic detection might be impossible. Integral counting (and therefore very high data rates) can be used for these observations.

I. INTRODUCTION

Much information on hydrogenlike impurities in semiconductors has been obtained from muon-spin rotation and/or resonance and/or relaxation (μSR) experiments on muonium, an unstable pseudoisotope of hydrogen where the proton is replaced by a positive muon (μ^+).[1] Recently, a variant of the μSR technique, muon level-crossing resonance spectroscopy (μLCR), has provided additional data on this subject, especially regarding muon bonding sites in semiconductors.[2] Two very distinct paramagnetic muonium states have been identified in the elemental semiconductors diamond, silicon, and germanium, as well as in the III-V compounds GaAs and GaP: *Normal muonium* (Mu), characterized by an isotropic hyperfine interaction (of roughly half the vacuum value), and *anomalous muonium* (Mu^*), exhibiting axial symmetry. Considerable theoretical[3] and experimental[2] effort has been devoted to elucidating the structures of these muonium states, especially in Si. Based on qualitative arguments a bond-centered (BC) model, in which Mu^* occupies a bond-centered position midway between the Si atoms, was proposed for Mu^* in Si.[4] An experiment where the ^{29}Si hyperfine structure was unambiguously resolved verified that Mu^* occupies the BC site.[5]

In this paper, we investigate the longitudinal-magnetic-field dependence of muon polarization for bond-centered Mu^* in polycrystalline material, and show that it exhibits nonmonotonic behavior. General analytic expressions for this field dependence (valid for all but

very low fields) are derived in terms of the Mu* hyperfine parameters.[6] The quantitative predictions for Si are experimentally confirmed in the appropriate temperature range. Such a distinctive signature should allow observation of Mu* or similar molecular radical states in other disordered solids, where conventional transverse-field μSR spectra would be broadened beyond detection. The application of this method to *amorphous* semiconductors might be especially fruitful.

II. THEORY

The spin Hamiltonian for Mu* in an external field B directed along the z axis can be written as

$$H=h\nu\mathbf{I}\cdot\mathbf{S}+h\delta\mathbf{I}\cdot\mathbf{n}\mathbf{S}\cdot\mathbf{n}-g_\mu\mu_\mu BI^z+g_e\mu_e BS^z \ . \tag{1}$$

The hyperfine interaction between the muon spin $\mathbf{I}$ and the electron spin $\mathbf{S}$ from the first term is isotropic. The second term produces an anisotropic hyperfine interaction with the unit vector $\mathbf{n}$ pointing along one of $\langle 1,1,1\rangle$ axes. For bond-centered Mu* in polycrystalline material, the longitudinal muon polarization exhibits a nonmonotonic field dependence with a discontinuity in the slope occurring at some particular field value B_ν, as will be shown below. For most of the substances in which the formation of Mu* has been observed, B_ν is in a field region of order several hundred mT. In this case, the spin dynamics, which is governed by the Hamiltonian [Eq. (1)], is extremely well approximated by assuming that states with the electron spin parallel and antiparallel to the field are practically decoupled.[7] This allows an analytic calculation of the time dependence of the polarization function in terms of two effective spin-Hamiltonian operators

$$H_\pm=\pm\tfrac{1}{2}h\nu I^z\pm\tfrac{1}{2}h\delta\mathbf{I}\cdot\mathbf{n}n^z-g_\mu\mu_\mu BI^z \ . \tag{2}$$

They describe the Larmor precession of the muon in an effective field given by

$$H_\pm=-g_\mu\mu_\mu\mathbf{I}\cdot\mathbf{B}_{\mathrm{eff},\pm} \ , \tag{3}$$

with components

$$B^x_{\mathrm{eff},\pm}=\mp\frac{h\delta}{2\gamma_\mu}\sin\theta\cos\theta \ , \tag{4}$$

$$B^z_{\mathrm{eff},\pm}=B\mp\frac{h\nu}{2\gamma_\mu}\mp\frac{h\delta}{2\gamma_\mu}\cos^2\theta \ ; \tag{5}$$

the axes being chosen so that z is the external field direction and $n^y=0$. Here, $\gamma_\mu=g_\mu\mu_\mu\cong 135.5$ MHz/T denotes the gyromagnetic ratio of the muon and θ is the angle between the symmetry axis of Mu* and the external field.

For the following, it is convenient to introduce the magnetic fields

$$B_\nu\equiv-\frac{h\nu}{2\gamma_\mu} \tag{6}$$

and

$$B_\delta\equiv\frac{h\delta}{2\gamma_\mu} \ , \tag{7}$$

and their ratio

$$\mu\equiv\frac{B_\nu}{B_\delta} \ , \tag{8}$$

as well as the reduced field

$$\beta\equiv\frac{B-B_\nu}{B_\delta} \ . \tag{9}$$

For convenience, their values for the elemental semiconductors are given in Table I. The components of the effective field are then given by

$$B^x_{\mathrm{eff},\pm}=\mp B_\delta\sin\theta\cos\theta \tag{10}$$

and

$$B^z_{\mathrm{eff},\pm}=B\pm B_\nu\mp B_\delta\cos^2\theta \ . \tag{11}$$

The time-independent contribution to the longitudinal polarization (μ^+ polarization along direction of externally applied magnetic field) is then

$$p(\theta)=p_+(\theta)+p_-(\theta) \ , \tag{12}$$

where

$$p_\pm(\theta)=\tfrac{1}{2}\frac{(B^z_{\mathrm{eff},\pm})^2}{(B^x_{\mathrm{eff},\pm})^2+(B^z_{\mathrm{eff},\pm})^2} \ ; \tag{13}$$

the time-dependent contribution becomes completely negligible when the average over directions is taken. With our sign convention, the contribution

$$p_-(\theta)=\tfrac{1}{2}-\tfrac{1}{2}\frac{\sin^2\theta\cos^2\theta}{\beta^2+(1+2\beta)\cos^2\theta} \tag{14}$$

exhibits the interesting peculiar field dependence. For a polycrystalline sample, the average over all angles gives

$$\langle p_-\rangle=\frac{1}{2}-\frac{1}{2}\frac{1}{1+2\beta}\left[\frac{2}{3}-F^2-F(1-F^2)^{\frac{1}{2}}\ln\left|\frac{1+F}{1-F}\right|\right] \ ,$$

$$\text{for } -\mu\le\beta\le-\tfrac{1}{2} \tag{15}$$

and

$$\langle p_-\rangle=\frac{1}{2}-\frac{1}{2}\frac{1}{1+2\beta}\left[\frac{2}{3}+F^2-F(1+F^2)\arctan\frac{1}{F}\right] \ ,$$

$$\text{for } -\tfrac{1}{2}\le\beta \ , \tag{16}$$

with the abbreviation

TABLE I. Experimental values of the hyperfine parameters $\nu=A_\perp$ and $\delta=A_\parallel-A_\perp$ for anomalous muonium in the elemental semiconductors (from Ref. 2), the corresponding fields B_ν and B_δ and their ratio $\mu\equiv B_\nu/B_\delta$.

	ν (MHz)	δ (MHz)	B_ν (T)	B_δ (T)	μ
C	−392.55	560.57	1.4485	2.0685	0.700
Si	−92.59	75.77	0.3417	0.2796	1.220
Ge	−131.04	103.77	0.4835	0.3829	1.261

$$F^2 \equiv \frac{\beta^2}{|1+2\beta|} . \tag{17}$$

At $\beta=-0.5$, the value of $\langle p_- \rangle$ is 7/30.

The polarization $\langle p_- \rangle$ is a universal function of the reduced field β and is shown in Fig. 1. The abrupt change in the slope at $\beta=0$ is of particular interest because it is an easily measurable signature of Mu*. At this field value, the z component as well as the x component of the effective field $B_{\text{eff},-}$ vanishes for $\theta=90°$. A Mu* center with exactly $\theta=90°$ gives a constant contribution of practically 0.5 to the longitudinal polarization around $\beta=0$, since the initially formed states are eigenstates of H. The centers *around* $\theta=90°$, which contribute dominantly to the polycrystalline average, exhibit an oscillation with frequency that changes sign at $\beta=0$. A series expansion around $\beta=0$ leads to the expression

$$\langle p_- \rangle = \tfrac{1}{6} + \tfrac{2}{3}\beta + \frac{\pi}{4}|\beta| . \tag{18}$$

It should be noted that the total polarization contains also the term $\langle p_+ \rangle$, in addition to $\langle p_- \rangle$. Around $\beta=0$ this term is, however, a monotonically increasing function of β and is given by

$$\langle p_+ \rangle = \frac{1}{2} + \frac{1}{2}\frac{G^2}{(\beta+2\mu)^2} \times \left[\frac{2}{3} - G^2 - G(1-G^2)^{\frac{1}{2}} \ln \left| \frac{1+G}{1-G} \right| \right] , \tag{19}$$

where

$$G^2 = \frac{(\beta+2\mu)^2}{2\beta+4\mu-1} . \tag{20}$$

We emphasize that this peculiar behavior of the longitudinal polarization is not an artifact of the approximations introduced by the effective Hamiltonian [Eq. (2)]. Shown in Fig. 2 is the field dependence of the polarization for Si, calculated using the full Hamiltonian [Eq. (1)] for a random selection of 1000 different directions **n** for every field value considered. (As in the analytic approximation, the time-dependent contribution is negligible and has been omitted.) This shows that the approximation of the spin Hamiltonian by Eq. (2) is appropriate for all but low-field values. These expressions describe a distinctive variation of polarization over an extended range of magnetic field, in addition to the sharp cusp. It is instructive to relate this broad variation to the narrower feature associated with Mu* in single-crystal Si and with a variety of muonium-substituted molecular radicals in organic solids. Such features occur in the close vicinity of a crossing of two energy levels of the system. No loss of polarization at the "zero crossing" occurs in systems with purely isotropic hyperfine coupling because the relevant levels cross exactly with no mixing of the spin states. Anisotropy removes the degeneracy so that crossing is avoided, the states are mixed, and polarization is lost near the (avoided) crossing. For Mu* with its axial anisotropy, there are actual crossings for $\theta=0°$ and 90°, sometimes referred to as *zero crossings* since the μ^+ precession frequency goes to zero at these crossings. These zero-crossing resonances (ZCR) can be seen in normal muon level-crossing resonance experiments most clearly when θ is close to but not equal to 0° or 90°. They are also termed $\Delta M=1$ avoided level crossings where M is the sum of the magnetic quantum numbers for the muon and nuclear spins (the latter is not involved in this case). The cusp in the polarization for a crystalline powder results from the angular average of the $\theta=90°$ ZCR. Numerical simulations for molecular radicals in powders also show this cusp.[8]

In molecular radicals, the anisotropy terms rarely exceed 10% of the isotropic coupling, leading to correspondingly narrower resonances. It is the extreme anisotropy of the Mu* hyperfine tensor, where the isotropic or contact term is comparable with the pseudodipolar or traceless components, which leads to the extended variation of polarization with field. The variation may in this

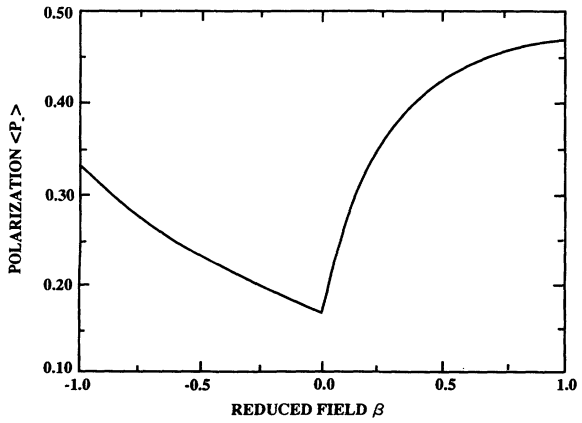

FIG. 1. Polarization $\langle p_- \rangle$ as a function of reduced field β.

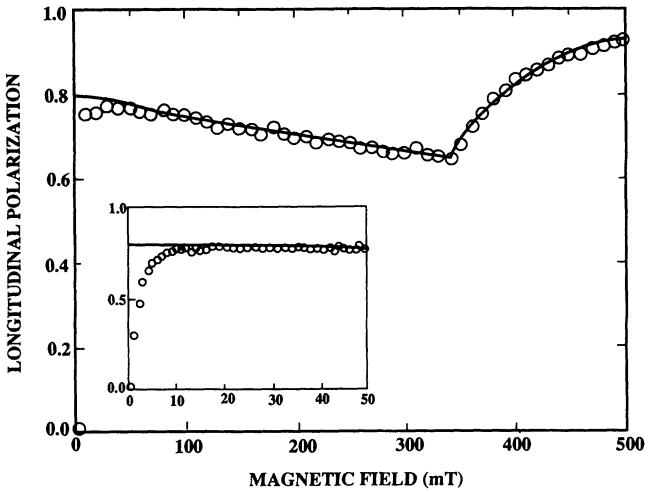

FIG. 2. Longitudinal polarization vs field for polycrystalline Si calculated with the full spin Hamiltonian (Eq. 1). The values were obtained by sampling over 1000 random directions **n**. The solid line is the approximate result $\langle p \rangle$. The inset shows the deviations occurring at low fields.

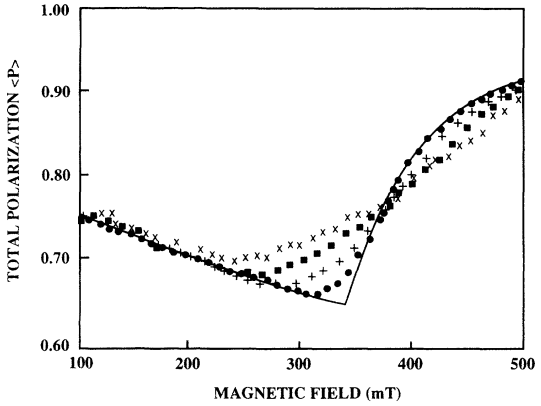

FIG. 3. Total polarization $\langle p \rangle$ as a function of field for polycrystalline Si calculated for a uniform distribution of hyperfine-parameter values between the indicated limits: $\pm m\%$ around ν and $\pm m\%$ around δ, where $m = 10$ (●), 20 (+), 30 (■), and 40 (×).

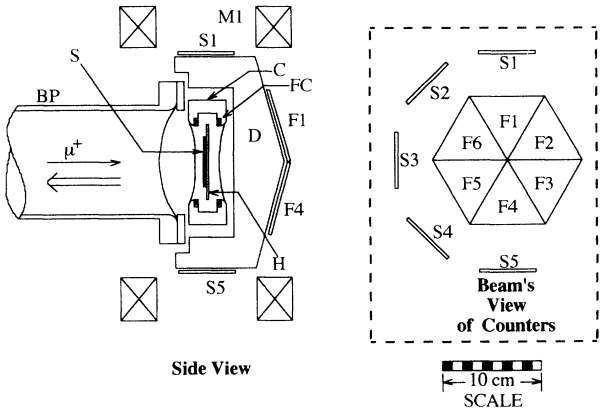

FIG. 4. μLCR spectrometer. *S*, sample; *H*, sample holder; *C*, cryostat; *D*, Al degrader; *S*1-5, side positron counters; *F*1-6, downstream positron counters; *M*1, scan coils; FC, flux coils; BP, beam pipe. The 500 mT coils are not shown. Auxiliary transverse coils (not shown) produce a field that is normal to the plane of the side view. The single arrow indicates μ^+ momentum, which is opposite the μ^+ spin (double-line arrow).

sense be understood as the powder pattern of level-crossing resonances.

This unusual field dependence of the longitudinal-muon-polarization function represents a distinct signature of Mu* in polycrystalline material, and can be used to study the thermal destruction of such centers. Furthermore, it may also be useful for the study of Mu* in amorphous samples. Shown in Fig. 3 are the results of simulations for which a spread of the hyperfine-parameter values around the crystalline values is assumed. It is seen that the onset of the rise of the polarization is shifted towards lower field values as the spread of the distribution of the hyperfine-parameter value ν is increased.

III. EXPERIMENT

The validity of the analytical expression, and of the magnitude of the cusp field B_ν in silicon, has been tested in experiments done at LAMPF, using the recently commissioned high-flux μLCR spectrometer.[9] The sample used was high-purity Si, supplied as a wafer but ground to a fine powder for the purposes of these experiments.[10] Measurements of the longitudinal muon polarization were made in field scans up to 500 mT and at two temperatures, 53 and 200 K. At the lower temperature, the anisotropic Mu* state is known to coexist with the isotropic Mu state. At the higher, only Mu survives as a paramagnetic state, Mu* being ionized to a diamagnetic state (with field-independent polarization).[1] The cusp characteristic of the Mu* state is, therefore, only expected to be visible in the lower temperature data.

With the new LAMPF spectrometer, polarization is obtained from the ratio in positron counting rate between downstream and side arrays of detectors (see Fig. 4). The problem of distorted data due to high positron rates is ameliorated by segmenting each array and by placing Al degraders in front of each detector. This preserves signal-to-noise ratio at reduced counting rate by selection of the higher energy positrons. Data are accumulated in the "integral-counting" mode, i.e., with no time correlation between incoming muons and outgoing positrons. This allows the full intensity (2×10^7 μ^+/sec average) of the LAMPF surface muon beam to be used.

In longitudinal-field experiments (magnetic field applied along direction of μ^+ spin), an absolute calibration of polarization is usually obtained from the amplitude of a muon-spin *rotation* signal, recorded on a standard sample by applying an auxiliary transverse field.[11] This requires time-resolved data acquisition. A variant of this procedure, without time resolution, and therefore suitable for integral counting, uses the so-called Hanle signal.[12] In this method, the ratio of the integral positron counting rates of detectors at different angles is monitored as the auxiliary transverse field is swept either side of zero. In the present geometry, the ratio of the sum of positron counts in the front (downstream) counters to the sum of positron counts in the side counters is minimal at zero field for the surface beam used, while at high transverse field ($\gg 0.5$ mT) rapid spin precession leads to effectively complete depolarization and hence the ratio approaches a constant larger value. Note that the μ^+ spin is opposite the momentum, as shown in Fig. 4. The variation of this ratio is an absolute calibration of the polarization. Such a calibration was performed with a pure aluminum sample at ambient temperature, for which the muon depolarization is negligible.

The distinctive Mu* cusp at 340(5) mT is clearly visible in Fig. 5 for the 53-K data of polycrystalline Si, thus confirming the prediction of Sec. II. At this temperature, the detailed field dependence of the polarization is the sum of the "repolarization" curves for the coexistent Mu and Mu* states. The precise shape of the measured curves, however, depends on the response function of the spectrometer, since both the positron orbits and the pho-

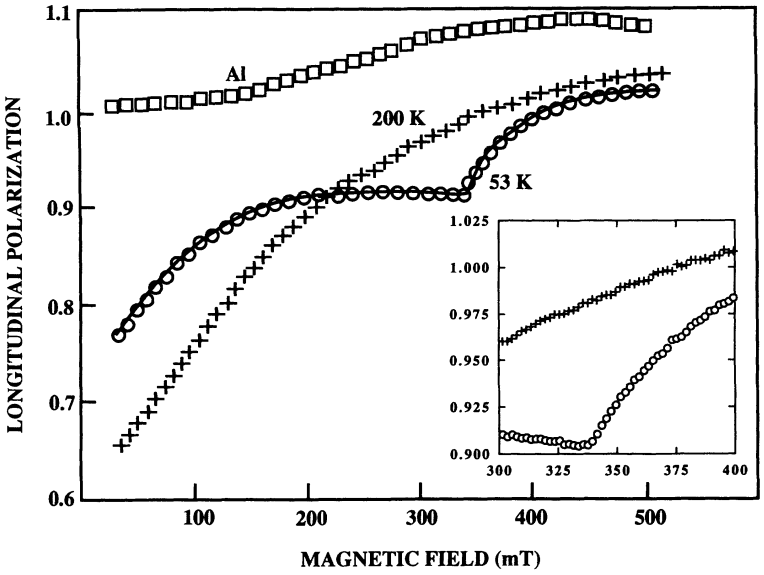

FIG. 5. Experimental polarization for polycrystalline silicon (symbols are from measurements and the solid line is from a fit to the 53-K data). The inset shows expanded data between 300 and 400 mT.

totube efficiencies are affected by the applied magnetic field. There will also be some dependence on the sample shape, size, and thickness. Data, collected as a series of limited field (40 mT), overlapping sweeps and then pieced together in the overlap regions, are presented in Fig. 5, with the polarization scale established by the Hanle calibration using Al. It was not convenient to scan the entire 500-mT field range. Although this procedure is expected to remove most of the instrumental effect, it is obvious from the Al data of Fig. 5 that there is a systematic error in this method. There is no depolarization of Al in this field range, and therefore, its polarization should be constant and equal to 1.0; however, the data exhibit polarization that increases with magnetic field and approaches magnitude 1.1.

Data obtained at 53 K in the 0–500-mT field region have been fitted to extract the fractional components of Mu, Mu*, and μ^+. A preliminary fit implied that a fourth signal (additional component) was also present at this temperature. Because the sample was ground and stored in air, it is expected to have an oxide coating, and thus it is possible that some fraction of the rapidly diffusing Mu reaches the surface of each Si crystallite and produces a signal characteristic of SiO_2. Consequently, the data were fitted to four signals with hyperfine constants fixed to the appropriate values for Mu, Mu* and Mu in Si, and Mu in SiO_2. With no requirement that the fractions sum to 1.0, the best fit yielded 0.38 Mu, 0.36 Mu*, 0.19 μ^+ in Si, and 0.12 Mu in SiO_2, and is shown as the solid line in Fig. 5. These fractions can be compared to low-temperature, zero-time values of 0.56 Mu, 0.39 Mu*, and 0.06 μ^+ in Si from standard time-differential μSR measurements on similar intrinsic crystals. This represents reasonable agreement when one adds the surface fraction to the diffusing Mu component and considers that ionization of either neutral species will contribute to the μ^+ fraction in a time-integral measurement. It should be noted that the data were fitted without attempting to make any correction for the distortion of polarization exhibited by the Al data (Fig. 5).

Several factors impede fitting the 200-K data. There are dynamic effects that contribute to the difficulty of making an accurate determination of initial fractions in Si at this temperature, e.g., muon state changes on the time scale of the muon lifetime (2.2 μs) and depolarization processes. Both effects begin to become important above roughly 100 K.[1] Specifically, time-differential longitudinal-field μSR measurements on this sample show no appreciable depolarization during the muon lifetime at 53 K; however, this is not true at 200 K.[13] Here it is important to make the distinction between *time-integral* longitudinal-field measurements (the data of Fig. 5) and *time-differential* longitudinal measurements. Integral techniques measure a quantity that is proportional to the integral of $P(t)$ averaged over the muon lifetime, whereas differential methods measure $P(t)$. With the assumption that relaxation at 200 K can be described by a single exponential, one can write $P(t)=P(0)\exp(-t/T_1)$, so that integral counting gives $P(0)[T_1/(\tau_\mu+T_1)]$ rather than $P(0)$. Conversely, the lack of significant time-differential longitudinal depolarization at 53 K implies that $P(t)\approx P(0)$. The relaxation at 200 K is quenched as the magnetic field is increased above the hyperfine field, the net effect being to distort the shape of the measured polarization curve, especially in the region around the hyperfine field value. Thus, no reasonable values for the various muon fractions can be extracted from the 200-K data. This fact does not, however, impact the main feature of the present work. The important information in the 200-K data for the present application is the *complete absence of a cusp at 340 mT,* clearly indicating a negligible Mu* fraction at that temperature, as expected.

IV. CONCLUSIONS

The experimental results presented here unambiguously demonstrate the existence of a cusp in the longitudinal

field dependence for Mu* in polycrystalline Si, as predicted. The lower temperature data also show that when dynamic effects such as state changes or depolarization processes are absent, semiquantitative information on the muon fractions can be extracted from this type of measurement. Given the instrument response function and a model of dynamic processes, it should be possible to obtain quantitative information. Time-integral measurements of the longitudinal field dependence of muon-spin polarization can provide an unambiguous identification of anisotropic muonium states. Under appropriate conditions such "repolarization curves" can yield quantitative results for fractions of the muon species present. This method, therefore, provides a means to investigate muonium centers having substantial anisotropy in a large class of materials for which sufficiently large, high-quality single crystals are not available.

ACKNOWLEDGMENTS

Work at Los Alamos is supported by the U.S. DOE. E.A.D. acknowledges financial support from the SERC (UK). The research of T.L.E. and B.H. was supported by NSF Grant Nos. DMR-8917639 and DMR-9220521 and Welch Foundation Grant No. C-1048 (T.L.E.). R.L.L. acknowledges research support from the Welch Foundation (Grant No. D-1053). A.M.S. acknowledges support from an AWU-DOE program.

[1]B. D. Patterson, Rev. Mod. Phys. **60**, 69 (1988).

[2]T. L. Estle *et al.*, in *Impurities, Defects and Diffusion in Semiconductors: Bulk and Layered Structures,* edited by D. J. Wolford, J. Bernholc, and E. E. Haller, MRS Symposia Proceeding No. 163 (Materials Research Society, Pittsburgh, 1990), p. 407; R. F. Kiefl and T. L. Estle, in *Hydrogen in Semiconductors,* edited by J. I. Pankove and N. M. Johnson (Academic, New York, 1991), p. 547.

[3]C. G. Van de Walle, in *Hydrogen in Semiconductors,* edited by J. I. Pankove and N. M. Johnson (Academic, New York, 1991), p. 585.

[4]S. F. J. Cox and M. C. R. Symons, Chem. Phys. Lett. **126**, 516 (1986).

[5]R. F. Kiefl *et al.*, Phys. Rev. Lett. **60**, 224 (1988).

[6]These analytic expressions were discussed briefly by P. F. Meier, *Proceedings of μSR-93-Maui, Maui, Hawaii, 1993* [Hyperfine Interact. (to be published)].

[7]P. F. Meier, in *Exotic Atoms '79,* edited by K. Crowe, J. Duclos, G. Fiorentint, and G. Torelli (Plenum, New York, 1979); A. Hinterman *et al.*, Am. J. Phys. **48**, 956 (1980).

[8]E. Roduner, Hyperfine Interact. **65**, 857 (1990).

[9]M. A. Paciotti *et al.*, *Proceedings of μSR-93-Maui, Maui, Hawaii, 1993* [Hyperfine Interact. (to be published)].

[10]E. A. Davis *et al.*, J. Non-Cryst. Solids **137&138**, 17 (1991).

[11]S. F. J. Cox, J. Phys. C **20**, 3187 (1987).

[12]M. A. Paciotti *et al.*, IEEE Trans. Nucl. Sci. **NS-32**, 3338 (1985).

[13]S. F. J. Cox *et al.*, Hyperfine Interact. **64**, 551 (1990).